

Grain boundary chromium depletion in austenitic alloys

Youfa Yin · Roy G. Faulkner · Paul Moreton ·
Ian Armson · Peter Coyle

Received: 25 February 2010 / Accepted: 26 May 2010 / Published online: 13 July 2010
© Springer Science+Business Media, LLC 2010

Abstract It is widely accepted that thermally induced grain boundary chromium depletion in austenitic alloys such as austenitic stainless steels and Ni base alloys can lead to inter-granular stress corrosion cracking (IGSCC) of high temperature components during service. Numerous experimental studies of the phenomenon have been reported and many models have been developed to predict chromium depletion under different pre-service treatment. However, there are debates on some fundamental issues in modelling and the interpretation of experimental observations. This article attempts to clarify some of the issues through numerical calculations and examination of the literature on grain boundary chromium depletion.

Introduction

Inter-granular stress corrosion cracking (IGSCC) and inter-granular attack (IGA) have been an issue of concern in high temperature pressurised water reactor (PWR) tubing components made from austenitic alloys, such as austenitic stainless steels and nickel base alloys, for many years. Chromium depletion from grain boundaries in these alloys due to the formation of grain boundary Cr-rich carbides, such as $M_{23}C_6$ and M_7C_3 , is known to be responsible for IGSCC, though the behaviour of the chromium depleted zones in nickel base alloys and stainless steels may be different due to the different base of the materials. The alloy development

approach to minimise this problem seems to be either reducing the carbon content of the alloy (e.g. from 304, 316 to 304L, 316L) thereby reducing the Cr-rich carbide formed or increasing the chromium content (e.g. from Inconel 600 to 690). However, processing of the material plays an important role as well. A good example is the application of heat treated Inconel 600 (Inconel 600TT) instead of mill annealed (Inconel 600MA). For a given composition of the material, the processing procedure and service conditions determine the precipitation kinetics and the amount of phases formed. Consequently, they determine the grain boundary chemistry. There are many experimental studies on the effect of processing, especially heat treatment, on Cr depletion from grain boundaries. For example, Kai et al. [1–3] have published detailed investigations of grain boundary Cr depletion profiles and the evolution of grain boundary Cr content in both Inconel 600 and 690 heat treated at various temperatures for a series of time durations. Experimental observations on stainless steels, such as 304 and 316, are also widely available [4, 5]. In order to be able to predict the effects of processing procedure on grain boundary Cr depletion and therefore the susceptibility to IGSCC of austenitic alloys, various computer modelling techniques have been developed by a number of groups and many of them have been demonstrated to be able to predict grain boundary Cr depletion profiles very well [6–11]. However, there is some debate on the Cr depletion mechanism. In this article, attempts are made to clarify some of the issues through numerical calculations and examination of the literature on grain boundary chromium depletion. A new model for predicting carbide interfacial Cr concentration has been proposed and is compared with some existing models.

At this point, some comment needs to be made about sensitivity arguments used in the context of nickel based alloys. It is acknowledged that normal sensitisation applies

Y. Yin (✉) · R. G. Faulkner
Department of Materials, Loughborough University,
Loughborough, Leicestershire LE11 3TU, UK
e-mail: y.yin@lboro.ac.uk

P. Moreton · I. Armson · P. Coyle
Rolls-Royce, P.O. Box 2000, Derby DE21 7XX, UK

to the reduction in passivation of iron due to the reduced chromium concentration at the grain boundaries. Clearly this applies strictly when iron is present in proportions of 60–70%, as is the case for austenitic steels. Since there is only approximately 10% iron in the Inconel alloys, other rapid grain boundary corrosion mechanisms must be at work. Rapid corrosion mechanisms undoubtedly occur in Inconel alloys because these alloys suffer accelerated grain boundary attack in acidic solutions [12] and this attack has been related to Cr depletion at the grain boundaries.

A clue to the alternative mechanisms can be found in the work of Thomas [13] where the electron microscope was used to view structure and composition in the grain boundary crack tip regions. Complex oxides of nickel and iron were observed, and so it is clear that nickel can also become more sensitive to oxidation in regions where Cr is depleted. This is the reason why in this article we propose that grain boundary Cr depletion is equally important for inter-granular sensitisation in both austenitic steels and nickel based alloys.

Review of theory

The reaction theory

It is commonly accepted that grain boundary Cr depletion and thereby the susceptibility to IGSCC of austenitic alloys are often related to grain boundary Cr-rich carbide precipitation. Therefore, one common description and explanation of the Cr depletion phenomenon is based on the precipitation reaction of the carbides (referred to as the reaction theory thereafter). The models developed by Stawström and Hillert [6], Was and Kruger [7] and Bruemmer [8] are representative examples of this theory and have been applied successfully in analysing grain boundary Cr depletion profiles. The basic theories are summarised below.

For a reaction of the form:



the following equation exists [8]:

$$\frac{[A_iB_j]}{[A]^i[B]^j} = K. \tag{2}$$

where [X] stands for the activity of X and K is a temperature dependent constant known as the solubility product. For precipitates A_iB_j under standard condition, the activity is unity. Therefore, the above equation can be simplified to:

$$[A]^i[B]^j = \frac{1}{K}. \tag{3}$$

In addition, the activity of an element is proportional to its concentration, $[A] = \gamma_A x_r^A$ and $[B] = \gamma_B x_r^B$. γ_A and γ_B are the activity coefficients and x_r^A and x_r^B are concentrations of

A and B, which are in thermodynamic equilibrium with the second phase, i.e. interfacial concentration rather than the bulk concentration. Therefore,

$$x_r^A = \frac{1}{\gamma_A [K(\gamma_B x_r^B)^j]^{1/i}}. \tag{4}$$

When Eq. 4 is applied to Cr-rich grain boundary carbides, A can be Cr and B is carbon, we have:

$$x_r^{Cr} = \frac{1}{\gamma_{Cr} [K(\gamma_C x_r^C)^j]^{1/i}} = \frac{1}{\gamma_{Cr} \gamma_C^{j/i} K^{1/i}} \frac{1}{(x_r^C)^{j/i}}. \tag{4a}$$

The interfacial Cr content is inversely proportional to the interfacial carbon concentration to the power of (j/i) . This means that interfacial Cr content increases as carbon concentration decreases.

It is well known that the diffusivity of carbon in austenitic alloys is several orders of magnitude higher than that of chromium. Therefore, it is commonly accepted that the distribution of carbon in a bulk material can be regarded as uniform throughout. The concentration of carbon is at maximum before any carbide precipitation takes place. As soon as any carbides form, they will take carbon from the matrix and carbon content in the matrix decreases. The decrease in carbon content continues until the equilibrium state is reached and the carbon content is equal to the solubility limit. As carbon concentration is uniform in the material, the same situation holds for grain boundaries as well. According to Eq. 4a, the grain boundary chromium content therefore increases progressively due to the decreasing activity (or concentration) of carbon. Thus, it is concluded that grain boundary chromium content is at the minimum at the instant of grain boundary Cr-rich particle nucleation; it increases as the precipitation continues and approaches the maximum when the carbon content approaches its solubility limit. The self-healing or desensitisation is denoted by the grain boundary chromium concentration increasing to a certain critical level. Before self-healing, sensitisation or chromium depletion increases as the width of the depleted zone increases, though the minimum grain boundary chromium content increases (or the depth of the grain boundary chromium depleted zone decreases) all the time. This explanation is schematically shown in Fig. 1 where (a) presents chromium concentration profiles near grain boundaries as a function of time, showing the depth of the depleted zone decreases ($x_{m1} < x_{m2} < x_{m3}$), while the width first increases ($w_2 > w_1$) then decreases ($w_2 > w_3$) and (b) shows the depth of the chromium depleted zone decreases gradually with annealing time at all temperatures, h is a measure of grain size (after ref. [6]).

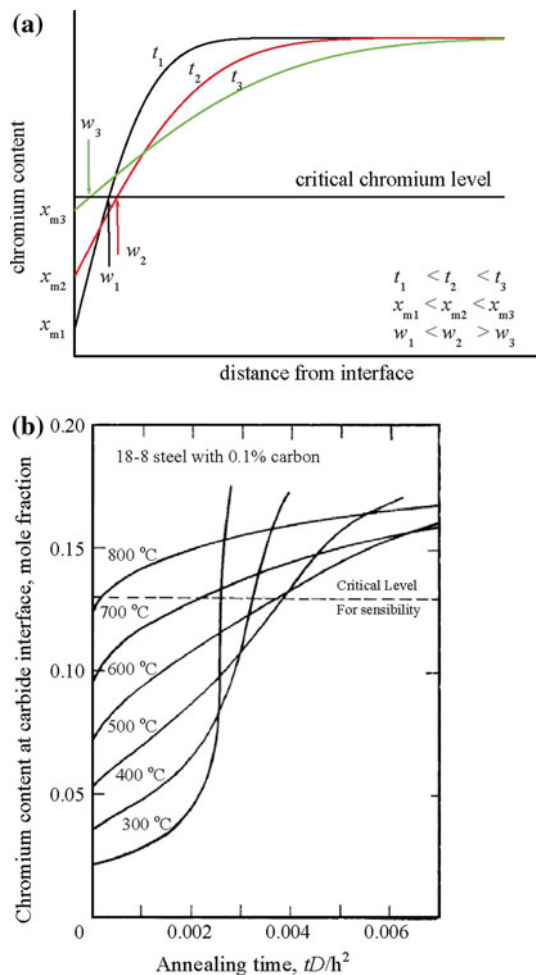


Fig. 1 Results of grain boundary chromium depletion according to the precipitation reaction theory

In summary, grain boundary Cr depletion is characterised by (1) the grain boundary chromium content is at the minimum at time $t = 0$, i.e. grain boundary chromium content increases as heat treatment time increases; (2) sensitisation and desensitisation are characterised by the width of the depleted zone alone, i.e. the wider the depleted zone, the more severe the sensitisation.

The kinetic theory

Experimental observations show that there is a delay in reaching the minimum chromium concentration, i.e. the minimum chromium concentration will only be reached after a finite time rather than at the beginning of precipitate growth [1, 2, 14–17]. Although one may argue that there are errors in the measured grain boundary chromium concentration due to effects such as electron beam broadening and shifting in transmission electron microscopy, the width of the chromium depleted zones compared to the size of common spot size used in determination of grain boundary

chromium concentration suggest that the delay in reaching the minimum is a real effect. It is important to realise that we are dealing with para-equilibrium. The thermodynamics dictate that the grain boundary Cr content should be constant at a given temperature, but it takes time for this situation to establish itself.

From a kinetic point of view, grain boundary chromium contents are determined by the amount taken by the grain boundary carbides and the amount diffused to the grain boundary from inside the grains. At earlier stages, carbides grow faster and the net result is a decrease of grain boundary Cr content. There is a point where carbide growth is sufficiently slow that the amount of Cr taken by grain boundary carbides is exactly balanced by that diffused to the boundary and the grain boundary Cr content reaches its minimum. After this point, the Cr diffused to grain boundaries exceeds that taken by the carbides and the net result is an increase in grain boundary Cr content. This is known as the kinetic theory. The phenomenon was realised many decades ago and is in agreement with the widely accepted depleted zone theory [18]. Recently, Sahlaoui et al. [9] and Yin and Faulkner [11] have proposed new approaches to model grain boundary chromium depletion based on this concept. For example, Yin and Faulkner claimed that their model can predict not only grain boundary chromium concentration profiles but also the evolution of the minimum grain boundary chromium content in agreement with experimental observations in Inconel 690. This interpretation of the grain boundary chromium depletion is illustrated in Fig. 2 where (a) shows chromium concentration profiles near grain boundaries showing both the depth and width of the depletion increase ($x_{m2} < x_{m1}$ and $w_2 > w_1$) and then decrease ($x_{m2} < x_{m3}$ and $w_2 > w_3$) with increasing heat treatment time; (b) grain boundary chromium concentration as a function of time at different temperatures showing the concentration decreases to a minimum and then increases gradually in Inconel 690 (after ref. [11]).

The Yin and Faulkner model [11] is based on the error function solution of diffusion law and Zener's relation of particle growth. The model has been successfully applied to Ni base alloys and austenitic stainless steels and has been shown to have some advantages over other existing models [19]. The grain boundary solute concentration is determined using the following equation [11]:

$$x_{GB} = \frac{\bar{x}V - 8kx_{max}}{V - 8k}, \quad (5)$$

where $V = (1 - V_f) V_0$ is the volume not occupied by the grain boundary carbides, V_0 the volume of the material considered, V_f the volume fraction of the precipitates, x_{GB} the grain boundary solute concentration, x_{max} the concentration far away from the grain boundaries. k is a

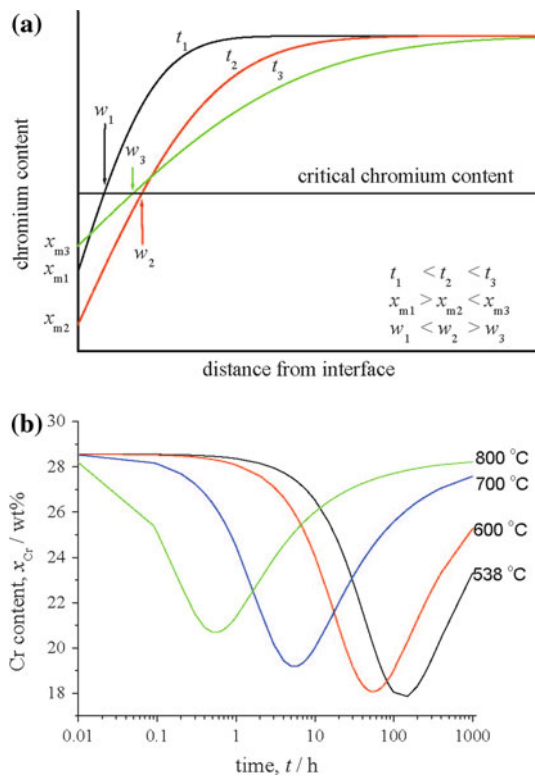


Fig. 2 Results of grain boundary depletion according to the precipitation kinetics theory

constant depends on the diffusivity and grain size according to the following equation:

$$k = \int_0^{a/2} \operatorname{erf}\left(\frac{x}{2\sqrt{Dt}}\right) dx \int_0^{b/2} \operatorname{erf}\left(\frac{y}{2\sqrt{Dt}}\right) dy \int_0^{c/2} \operatorname{erf}\left(\frac{z}{2\sqrt{Dt}}\right) dz, \tag{6}$$

where a , b and c are the three dimensions of the grain.

The average concentrations of the elements are determined by the initial concentration and the volume fraction of the precipitates. From mass conservation, the following relation holds,

$$x_0 \frac{V_0}{V_x} = \bar{x} \frac{V_0(1 - V_f)}{V_x} + N_s \frac{V_f V_0}{V_\theta}, \tag{7}$$

where N_s is the number of solute atoms in the molecule of the precipitates (e.g. 23 for Cr and 6 for C in Cr_{23}C_6). The left hand side of the equation is the total moles of solute atoms in the volume. The first term on the right hand side is the moles of solute remaining in the matrix, while the second term is the moles precipitated. Therefore,

$$\bar{x} = \left(x_0 - \frac{N_s V_f V_x}{V_\theta}\right) \frac{1}{1 - V_f}. \tag{8}$$

It is clear that the grain boundary chromium content can be determined if the volume fraction of carbides is known.

Yin and Faulkner [11] constructed a function to describe the dependence of volume fraction of precipitates on time based on Zener’s relation:

$$V_f = V_{f,\max} \frac{t^{3/2}}{t^{3/2} + t_{\max}^{3/2}}, \tag{9}$$

where $V_{f,\max}$ is the maximum volume fraction of the precipitates at the temperature of concern and t_{\max} is a material constant describing the kinetics of precipitation. Equation 9 satisfies the conditions that (1) $V_f = 0$ at $t = 0$; (2) $V_f = V_{f,\max}$ when $t \rightarrow \infty$. Figure 2b is generated using this theory.

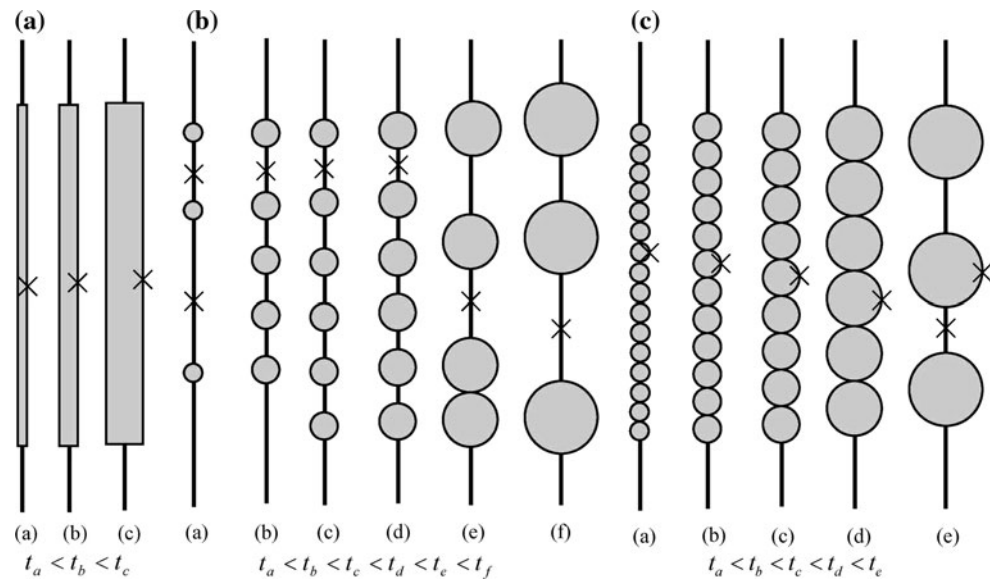
To summarise, the kinetic theory predicts (1) there is a delay in reaching the minimum grain boundary chromium concentration, i.e. grain boundary chromium concentration decreases and then increases with increasing heat treatment time; (2) the sensitisation and desensitisation is characterised by both the width and the depth of the depletion zone, i.e. the severest sensitisation occurs when both the depth and the width are at their maxima.

Limitations of existing models

One of the assumptions made in developing the reaction theory models is that the grain boundary is completely covered by a continuous layer of carbides with flat surface, i.e. a carbide film with uniform thickness as illustrated in Fig. 3a. Under such circumstances, the grain boundary chromium concentration as commonly referred to is actually the interfacial concentration at the carbide–matrix interface, that is, the concentration at locations marked with a cross in Fig. 3a. In contrast, the kinetic models, such as the Yin and Faulkner model, are dealing with a situation illustrated in Fig. 3b and the grain boundary chromium concentration referred to here is the chromium concentration between the adjacent grain boundary carbides, as marked with a cross in Fig. 3b. These two grain boundary chromium concentrations and their evolution with treatment time can be different.

Although many authors have compared the reaction theory model predictions with experimental measurements and have claimed the predictions are in good agreement with measured grain boundary chromium concentration profiles, this kind of comparison should be treated with care as experimental grain boundary chromium concentrations are measured at locations as indicated between adjacent grain boundary carbides as assumed in the Yin and Faulkner model. For example, Kai et al. [1, 2], Was et al. [7, 14], Bell et al. [5], and Bruemmer et al. [20] all specifically pointed out that the results they reported are made between adjacent carbides. Bruemmer et al. [20] emphasised that the profiles were measured between

Fig. 3 Grain boundary precipitate coverage. **a** The reaction theory model; **b** the kinetic theory model; **c** alternative complete grain boundary coverage to the reaction theory model



carbides that were more than one micron apart. Indeed, any direct measurement of interfacial chromium concentration is deemed to be interfered by the carbides and therefore any direct comparison with the reaction theory model will be difficult. This explains the inability of the reaction theory models to correctly predict the time delay in reaching the minimum grain boundary chromium concentration as reported by many authors mentioned in “[The reaction theory](#)” section and the good agreement have achieved by the kinetic models in predicting both grain boundary chromium concentration profiles and their evolution.

The reaction theory models discussed above have other shortcomings. As discussed above, the width of the chromium depleted zone is used to characterise if a boundary is sensitised without specific reference to the depth of the depleted zone in the reaction theory based models. As long as the depleted zone is wide enough for corrosive molecules, such as the sulphur-bearing species, which cause corrosion in the same manner to both stainless steels and nickel alloys and are products of the chemical reaction of sodium thiosulfate in acidic environments [2], to find a path to get into the material, the depth of the depleted zone determines the degree of corrosion within the path. Therefore, the depth of the depleted zone (or the minimum grain boundary chromium content) is more relevant to be used for characterising a grain boundary. Sourmail et al. [10] have recently pointed out that these models do not guarantee a flux balance of solute atoms to the carbides. Indeed, the flux of solute atoms to the grain boundaries and grain boundary carbides are not considered in the reaction theory models and this is the main difference from kinetic theory based models. Sourmail et al. [10] therefore proposed a model where carbon activity is calculated using a thermodynamic software, MTDATA, and the interfacial

chromium concentration is then obtained by solving the flux balance equations at the interface of carbides. As a complete coverage of grain boundary by a carbide film is still the basis of their model, the results are not in good agreement with experimental observations, though the model predicts the time delay in reaching the minimum interfacial chromium concentration.

It should be noted that both the interfacial and grain boundary chromium concentrations are important in considering susceptibility to inter-granular stress corrosion cracking if the grain boundary carbide distribution is discrete. In such a case, the possible paths for corrosive molecules to get deep into the material are carbide free grain boundary sections and the interface between grain boundary carbides and the matrix. The corrosion resistance of the former is determined by the grain boundary chromium concentration and the latter is determined by the interfacial chromium content. The grain boundary chromium concentration and its evolution can be predicted using the kinetic theory based models discussed above, such as the Yin and Faulkner model. The interfacial chromium concentration can be forecasted using the reaction theory based models. However, as the assumption that the grain boundary is covered by a thin carbide film has been used in all these models and the radius of curvature of grain boundary carbides is finite in the reality, a new model, which considers both capillary effect and flux balance of grain boundary carbides is desirable.

New model theory

The capillary effect of particles is an important phenomenon, which has to be considered in precipitation studies. It

has effects on the critical nucleus size (the interfacial solute concentration at the surface of the nuclei must be lower than that in the matrix) and particle coarsening. As Cr depletion is closely related to the grain boundary carbide precipitation, the capillary effect should also be considered in Cr depletion models.

The capillary effect is described by the well-known Gibbs–Thomson equation and one of the widely used forms is as follows [21]:

$$x_r = x_\infty \exp\left(\frac{2\gamma V_\theta}{rRT}\right) \tag{10}$$

where x_r is the interfacial concentration of a particle with radius of curvature of r , x_∞ is such a value when $r = \infty$ or as commonly referred to as the equilibrium concentration, γ the interfacial energy, V_θ the molar volume of the precipitate phase, R the universal gas constant and T the absolute temperature. However, this is only a simplified version. Generally, for a precipitate of the form $A_iB_jC_k\dots$, the general form of Gibbs–Thomson equation is [22]:

$$\exp\left[\frac{2\gamma V_\theta}{rRT}\right] = \left(\frac{x_r^A}{x_\infty^A}\right)^i \left(\frac{x_r^B}{x_\infty^B}\right)^j \left(\frac{x_r^C}{x_\infty^C}\right)^k \dots \tag{11}$$

The solubilities are related to each other via the solubility product equation:

$$(x_\infty^A)^i (x_\infty^B)^j (x_\infty^C)^k \dots = \exp\left(-\frac{\Delta H}{RT} + \frac{\Delta S}{R}\right) \tag{12}$$

where ΔH and ΔS are the formation enthalpy and entropy of the phase and can be determined using thermodynamic phase calculation software such as MTDATA and ThermoCalc or by experimental measurements. Therefore, the number of unknowns ($x_r^A, x_r^B, x_r^C, \dots$) in Eq. 11 is equal to the number of elements in the precipitate phase and therefore Eq. 11 is not enough to find all the unknowns alone even for the simplest binary systems. Fortunately, the growth of the precipitate particles requires that the amount of atoms of different elements diffusing to the particle must satisfy the ratio dictated by the chemical formula of the phase. This yields the commonly known flux balance equations:

$$dV_A = dV_B = dV_C = \dots \tag{13}$$

or

$$\frac{D_A(\bar{x}^A - x_r^A)}{\frac{V_\theta}{V_0}i - x_r^A} = \frac{D_B(\bar{x}^B - x_r^B)}{\frac{V_\theta}{V_0}j - x_r^B} = \frac{D_C(\bar{x}^C - x_r^C)}{\frac{V_\theta}{V_0}k - x_r^C} = \dots \tag{14}$$

where dV_A, dV_B and dV_C are volume increases due to the increase of elements A, B and C, respectively. D is the diffusivity, \bar{x} the average concentration and V_α the molar volume of the matrix. Equation 14 provides $n - 1$ independent equations (n is the number of elements in

the precipitate phase) and therefore can be used together with Eq. 11 to form a set of simultaneous equations. In principle, the set of equations can be solved for x_r and all the unknowns be found. However, the order of the equation is $i + j + k + \dots$ and therefore can only be solved analytically for very simple precipitates, such as MX ($M =$ metallic elements, $X = C$ or N) particles. For more complicated precipitates, such as $M_{23}C_6$ in common steels and Ni based alloys, numerical methods have to be used. For MX particles, as the diffusivity of carbon or nitrogen is several orders of magnitude higher than that of the metallic elements, their distribution can be regarded as uniform throughout the material and unrelated to the particle size, i.e. $x_\infty = x_r = \bar{x}$. In such a case, taking M as A and X as B , Eq. 11 yields

$$\exp\left[\frac{2\gamma V_\theta}{rRT}\right] = \left(\frac{x_r^M}{x_\infty^M}\right)^i \tag{15}$$

or

$$x_r^M = x_\infty^M \exp\left[\frac{2\gamma V_\theta}{irRT}\right] \tag{16}$$

Note that $i = 1$, and we have

$$x_r^M = x_\infty^M \exp\left[\frac{2\gamma V_\theta}{rRT}\right]. \tag{17}$$

This is equivalent to Eq. 10.

As discussed above, the interfacial solute concentration can be determined using Eqs. 11 and 14 provided that the average concentration of all elements is known. For the average solute concentration in the matrix, Eqs. 8 and 9 can be used. For particles with finite radius of curvature, the radius is also required to determine the interfacial concentration and is described using the Zener’s relation [23]:

$$r = \beta\sqrt{t} \tag{18}$$

where β is the growth rate.

This model provides an alternative to the reaction theory approach to predicting interfacial solute concentration with an advantage in the capability of the inclusion of the capillary effect.

Results

Interfacial concentration as a function of particle radius

The set of simultaneous equations formed according to Eqs. 11 and 14 for various types of precipitates have been solved using the Newton–Raphson approach. The forms of particles studied include AB, A_2B , ABC, A_7B_3 and $A_{23}B_6$ to represent some common phases in steels and Ni base

alloys such as VN (vanadium nitride), Laves Phase (Fe_2Mo), Z phase (CrNbN), carbides (Cr_7C_3 and Cr_{23}C_6). In all cases, the Newton–Raphson approach gives satisfactory solution when checked against the original equations and the exact solution for the simplest case of VN.

Figure 4 presents the results for VN where interfacial vanadium and nitrogen concentrations being plotted as a function of the radius of curvature. The symbols in the graph are exact solutions of the Gibbs–Thomson and flux balance equations using the Newton–Raphson approach for conditions shown in Table 1. Lines are plots of the simplified Gibbs–Thomson equation, Eq. 10. As commonly known, the diffusivity of nitrogen is a few orders of magnitude higher than that of vanadium and nitrogen can be considered as uniformly distributed. Figure 4 clearly demonstrates this point. The interfacial concentration of nitrogen (circles, right hand side axis) is practically the same at interfaces of particles with all radii of curvature and is equal to the average nitrogen concentration, 0.00211 or 2.11×10^{-3} in the figure. On the other hand, the interfacial vanadium concentration (squares, left hand side axis) clearly shows the capillary effects: interfacial concentration increases sharply with decreasing radius of curvature, especially when the radius of curvature is less than about 10 nm. For particles larger than 100 nm in radius, the capillary effects are small and may be neglected.

The lines in Fig. 4 are plots of Eq. 10 with x_∞ taken as the corresponding interfacial concentration with radius of curvature set to 10^5 nm or $100 \mu\text{m}$. For nitrogen (dashed line), the interfacial concentration predicted using Eq. 10 substantially differs from the exact solution. However, for vanadium (solid line), Eq. 10 applies very well. The parameters used are shown in Table 1. Note that figure 1.47 has been used for all elements as what really matters here is the order of magnitude of the diffusion coefficients.

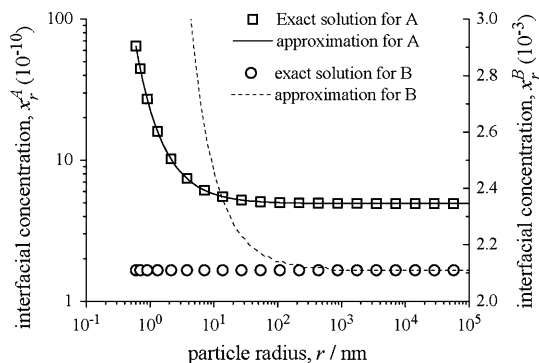


Fig. 4 Interfacial concentration of elements at the interface of type AB particle with vanadium nitride (VN, A = V; B = N) as an example

The same trends have been found for Cr_{23}C_6 (Fig. 5) where carbon diffuses much faster than chromium (see Table 1). In fact, the same situation applies to Cr_7C_3 and NbCrN as well. Therefore, it is concluded that when the diffusivities of the elements are substantially different, the interfacial concentration of the faster diffusing element is equal to the average, irrespective of the particle size, while that of the slower diffusing element(s) shows capillary effects and can be described by the simplified Gibbs–Thomson equation, Eq. 10 or more generally Eq. 16.

Figure 6 shows the solution for Laves Phase particles where the two main elements have similar diffusivities. The symbols are exact solutions of the Gibbs–Thomson and flux balance equations. The lines are plots of the simplified Gibbs–Thomson equation, Eq. 10. The simplified Gibbs–Thomson equation applies to neither of the two elements when the diffusivities are similar and the only way to find the interfacial concentrations is by solving the Gibbs–Thomson equation and the flux balance equations.

Interfacial concentration as a function of average concentration

Figure 7 shows the interfacial concentrations of chromium and carbon at the interfaces of M_{23}C_6 particles with sufficiently large radius ($100 \mu\text{m}$) of curvature (x_{inf}) as a function of the average carbon concentration in the matrix. The parameters used are the same as in Fig. 5 (see Table 1) except that the average carbon concentration varies. Symbols are exact solutions of the Gibbs–Thomson and flux balance equations. The dashed line ($x_{\text{inf}}^{\text{C}} = x_{\text{average}}^{\text{C}}$) is a plot of $x_{\text{inf}}^{\text{C}} = x_{\text{average}}^{\text{C}}$. The line labelled ($x_{\text{inf}}^{\text{M cal}}$) is the value of $x_{\text{inf}}^{\text{Cr}}$ calculated using the solubility product equation (Eq. 12). For carbon, $x_{\text{inf}}^{\text{C}}$ equals to (or more precisely slightly smaller than) the average carbon concentration until the equilibrium is reached and decreases when the average carbon concentration decreases. For chromium, $x_{\text{inf}}^{\text{Cr}}$ increases with decreasing average carbon concentration, in agreement with the conclusions from the reaction theory. The vertical dashed line indicates the true equilibrium state, while the vertical solid line represents a para-equilibrium state during the precipitation reaction. When the average carbon concentration decreases, the para-equilibrium approaches the true equilibrium state.

During precipitation process, the carbon concentration in the matrix decreases gradually due to the formation of carbide. At any instant, the system is in a para-equilibrium state where the interfacial concentrations at the carbide interface (of infinite radius of curvature) are governed by solubility product equation and can be determined using the vertical para-equilibrium concentration line in Fig. 6. As precipitation progresses, more and more carbon is taken by the carbides and average carbon concentration (or

Table 1 Parameters used in Figs. 4, 5, 6

Parameter (unit)	A	B	D_A (m ² s ⁻¹)	D_B (m ² s ⁻¹)	\bar{x}_A (at. fr)	\bar{x}_B (at. fr)	$\Delta H + T\Delta S$ (J mol ⁻¹)	T (K)	γ (J m ⁻²)	V_θ (m ³ mol ⁻¹)	V_α (m ³ mol ⁻¹)
Figure 4	V	N	1.47×10^{-18}	1.47×10^{-13}	0.0024	0.00211	200261	873	0.5	1.12×10^{-5}	9.05×10^{-6}
Figure 5	Cr	C	1.47×10^{-18}	1.47×10^{-13}	0.2	0.00611	883000	873	0.5	1.83×10^{-4}	9.05×10^{-6}
Figure 6	Fe	Mo	1.47×10^{-18}	1.47×10^{-18}	0.0024	0.00211	120000	873	0.5	1.68×10^{-5}	9.05×10^{-6}

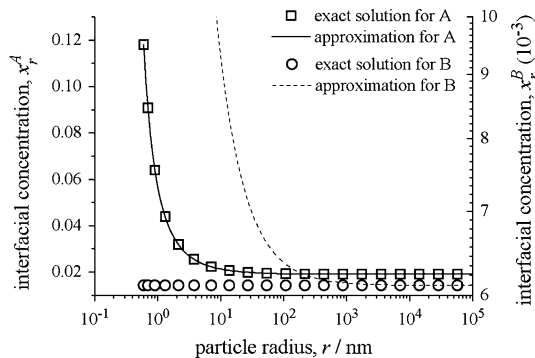


Fig. 5 Interfacial concentration of elements at the interface of type $A_{23}B_6$ particle with chromium carbide ($Cr_{23}C_6$, $A = Cr$; $B = C$) as an example

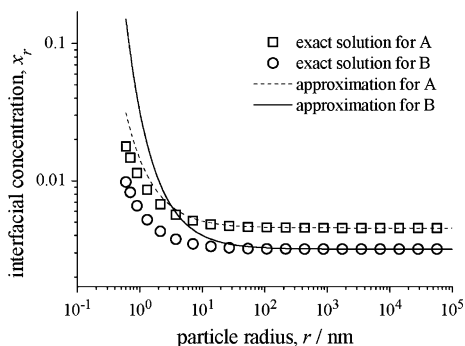


Fig. 6 Interfacial concentration of elements at the interface of type A_2B particle with laves phase (Fe_2Mo , $A = Fe$; $B = Mo$) as an example

activity) decreases. As a result, the interfacial chromium concentration increases gradually. This is the same as the results from the reaction theory, Eq. 4. When the volume fraction of carbides reaches its maximum, interfacial carbon concentration reaches its solubility limit and interfacial chromium concentration reaches a maximum. This is the final equilibrium state.

Interfacial and grain boundary concentration

The new model for predicting interfacial solute concentration in “New model theory” section has been applied to a nickel base alloy (Inconel 690, Ni–28.57% Cr–9.35% Fe) to model the interfacial chromium concentration at the

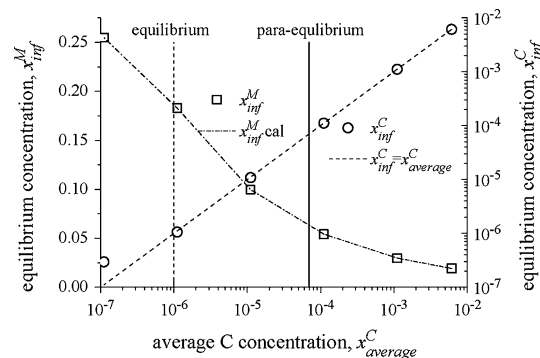


Fig. 7 Interfacial concentrations at interface of $M_{23}C_6$ particles with sufficiently large radius of curvature (x_{inf}^M) as a function of average carbon concentration

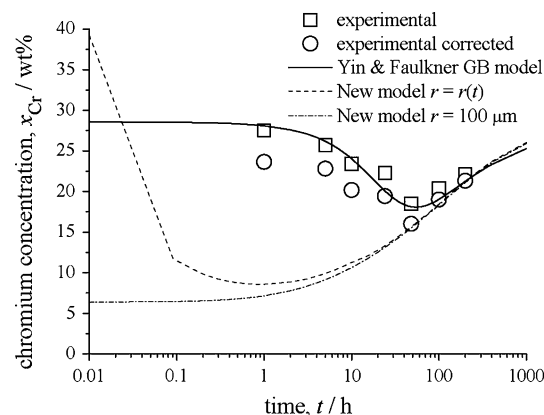


Fig. 8 Grain boundary/interfacial chromium concentration as a function of heat treatment time at 600 °C for a nickel base alloy, Inconel 690

interface of $M_{23}C_6$ as a function of heat treatment time. Figure 8 shows the results for a heat treatment temperature of 600 °C (dashed and dash-dotted lines), together with experimental measurements (symbols) after Kai et al. [1] and the predictions made by Yin and Faulkner (solid line) [11] using the grain boundary chromium depletion model also described here in “The kinetic theory” section. The para-equilibrium interfacial chromium concentration, as predicted by the new model with a particle radius of curvature of 100 μm (Fig. 8 dash-dotted line), is at a minimum at the beginning of precipitation and increases gradually with time as is expected from the reaction theory.

The rate of increase is dependent on the precipitation kinetics; that is the increase of volume fraction of the carbides. Although the longer term experimental measurements can be matched by adjusting the growth rate, the predictions are much lower than the experimental results at shorter times. When capillary effects exist, i.e. the radius of curvature of the particle increases gradually with increasing heat treatment time rather than being infinite right from the start of nucleation, the interfacial chromium concentration predicted using the new model (Fig. 8 dashed line) is very high at the beginning of precipitation. In fact, the nucleation theory states that the interfacial solute concentration at the surface of a particle of the critical size should not exceed the average solute concentration in the matrix. Therefore, at the start of precipitation, the interfacial solute concentration is close to the average. As the particle grows, the capillary effect decreases and there is a drop in interfacial chromium concentration. When the decrease in capillary effect is balanced by the increase in the para-equilibrium interfacial concentration, the interfacial chromium concentration reaches the minimum and then increases on further heat treatment. Although the inclusion of the capillary effect in the new model reveals the delay in reaching the minimum interfacial chromium concentration and gives higher interfacial chromium concentration at shorter times as compared to the para-equilibrium interfacial concentration, the drop in concentration is very sharp and the actual values of concentration are still much below the experimental measurements.

Discussion

The Gibbs–Thomson equation is essential to the understanding of the interfacial solute concentration and to precipitation kinetics modelling where it is used to calculate the interfacial solute concentration and subsequently the solute gradient at the surface of precipitates. Differences in interfacial solute concentration at larger and smaller particles due to the capillary effect are the driving force for the coarsening phenomenon in later stages of precipitation. Although the simplified Gibbs–Thomson equations are commonly used and referred to, the interfacial solute concentration should be determined generally by solving the simultaneous equations formed by the Gibbs–Thomson equation and the flux balance equations. With reasonable selection of the initial roots (such as the average concentrations), the simultaneous equations can be solved satisfactorily using the simple Newton–Raphson method. The simplified Gibbs–Thomson equations, Eqs. 10 and 16, can only be used if one of the elements in the formulation of the precipitates has substantially higher diffusivity than the others. In such a case, the interfacial solute

concentration of the slower diffusing element can be determined by taking the para-equilibrium interfacial concentration as x_{∞} rather than the final equilibrium interfacial concentration. This may be useful in modelling of various carbides and nitrides in austenitic alloys where carbon and nitrogen diffuse several orders of magnitude faster than the metallic components. Under such circumstances, the metallic components are the rate controller of the precipitation process and the growth of the particles can be calculated from the concentration gradient of the metallic components alone. However, for all intermetallics where all components are metallic elements and the diffusivities are similar, the interfacial concentrations must be found by solving the simultaneous equations.

It is commonly accepted that grain boundary chromium depletion in austenitic alloys is caused by the formation of grain boundary carbides, such $M_{23}C_6$ and M_7C_3 . Therefore, grain boundary chromium concentration is dependent on the grain boundary carbide coverage, volume fraction and intragranular carbide precipitation. Models for predicting grain boundary chromium depletion in austenitic alloys based on precipitation reaction theory, such as these by Stawström and Hillert [6], Was et al. [7] and Bruemmer [8], have difficulties in explaining the experimental measurements because the models predict a different chromium concentration as compared to that of experimental measurement, which is commonly made from scans on particle-free region of grain boundaries rather than across the surface of the carbides. The flat interface models predict no delays in reaching the minimum grain boundary chromium concentration. When the capillary effects are considered as in the new model for predicting the interfacial chromium concentration proposed in this article, the interfacial model predicts an initial drop in grain boundary chromium concentration. However, the delay in time is very short and the predicted interfacial chromium concentration at short times is much lower than experimentally measured grain boundary chromium content. Sourmail et al.'s predictions [10] for austenitic steels without the consideration of capillary effects are also much lower than experimental concentrations.

Nucleation theory states that the rate of nucleation is dependent on the saturation level, diffusivity and temperature. At low temperatures, nucleation may take a long time to complete. Therefore, it is natural to think that the particles are discrete at least at initial stages of precipitation and the distribution of particles becomes denser and denser as more nucleation takes place and the particles grow, as shown in Fig. 3b. As precipitation continues, the carbides may or may not form a continuous coverage of grain boundaries depending on the carbon content, nature of grain boundaries, grain size and temperature. For example, larger grain sizes give higher probability of forming a complete coverage while small grains may not

have sufficient carbon supply for the formation of a complete layer of grain boundary carbides. In the situations of discrete grain boundary carbide distributions, there are two chromium concentrations, which both are important to the inter-granular stress corrosion cracking. One is the interfacial chromium concentration at the interface of carbides, which can be predicted using the interfacial model described in this article (the new model proposed in this article). The other is the average chromium concentrations taken from particle-free boundaries, which has been referred to as grain boundary chromium concentration by Yin and Faulkner [11] and can be predicted using the Yin and Faulkner model described briefly in “The kinetic theory” section. The difference between the interfacial and grain boundary chromium concentrations implies that there is a chromium concentration gradient along grain boundaries required by the capillary effect. Therefore, the experimental measurements can vary with locations and are different in the interfacial and grain boundary regions.

The susceptibility of the grain boundaries to inter-granular stress corrosion cracking depends on the higher one of the two chromium concentrations. For a corrosive molecule to find the continuous path to the inner material through the grain boundary and particle–matrix interface linkage, both concentrations have to be lower than a critical level. From this point of view, sensitisation can be defined as when the higher of these two chromium concentrations are lower than the critical level and self-healing means this concentration becomes greater than the critical value.

Although it is not the scope of this article to discuss means to eliminate or to reduce the level of sensitisation in austenitic alloys, it should be mentioned that the grain boundary carbide coverage presented in Fig. 3 and grain boundary carbide precipitation kinetics can be affected greatly by grain size, grain boundary character distribution and grain boundary impurities. Therefore, grain boundary engineering approaches, which can be used to control grain size, grain boundary impurity and grain boundary character [24–29], can significantly change grain boundary chromium concentration evolution and consequently affect the susceptibility to IGSCC of the material. Studies on these effects are of great interest.

Conclusions

Intergranular stress corrosion cracking caused by grain boundary chromium depletion has been a concern in nuclear power plant austenitic stainless steels and nickel base alloys. This article provides a better understanding and a more accurate model of grain boundary chromium depletion in these alloys and related issues such as IGSCC and grain boundary carbide precipitation.

The interfacial solute concentrations at the interfaces of precipitates in austenitic alloys should be determined generally by solving the simultaneous equations formed by the Gibbs–Thomson equation and the flux balance equations as in the new model proposed in this article. In situations of carbides and nitrides, the interfacial concentration of the metallic component can be determined using the simplified Gibbs–Thomson equation without the need of solving the simultaneous equations. The interfacial carbon and nitrogen concentration is practically equal to the average and the para-equilibrium concentration of the metallic component can be determined from this average using the solubility product equation.

Distinction must be made between the interfacial chromium concentration at the interface of grain boundary carbides and the grain boundary chromium concentration measured at points between adjacent grain boundary carbides. The former can be predicted using the interfacial models proposed in this paper (the new model, kinetic theory based) and by others (the reaction theory model) while the latter can be forecasted using the Yin and Faulkner [11] grain boundary chromium depletion model which is also a kinetic model. If the grain boundary is completely covered by carbides, interfacial chromium concentration can be regarded as the grain boundary chromium concentration. In the case of discrete grain boundary carbides, both interfacial and grain boundary chromium concentration should be considered when considering grain boundary chromium depletion.

References

1. Kai JJ, Yu GP, Tsai CH, Liu MN, Yao SC (1989) *Metall Trans A* 20:2057
2. Kai JJ, Tsai CH, Huang TA, Liu MN (1989) *Metall Trans A* 20:1077
3. Kai JJ, Liu MN (1989) *Scr Metall* 23:17
4. Butler EP, Burke MG (1986) *Acta Metall* 34:557
5. Bell GEC, Tortorelli PF, Kenik EA, Klueh RL (1991) *J Nucl Mater* 179–181:615
6. Stawström C, Hillert M (1969) *J Iron Steel Inst* 207:77
7. Was GS, Kruger RM (1985) *Acta Metall* 33:841
8. Bruemmer SM (1990) *Corrosion* 46:698
9. Sahlaouia H, Sidhoma H, Philibert J (2002) *Acta Mater* 50:1383
10. Sourmail T, Too CH, Bhadeshia HKDH (2003) *ISIJ Int* 43:1814
11. Yin YF, Faulkner RG (2007) *Corros Sci* 49:2177
12. Yin YF, Faulkner RG (2010) Rolls-Royce internal annual report, May 2010
13. Thomas LE, Olszta MJ, Johnson BR, Bruemmer SM (2009) Abstracts of the 14th international conference on environmental degradation of materials in nuclear power systems, Virginia Beach, Virginia, USA, August 2009, p 20
14. Was GS, Tischner HH, Latanision RM (1981) *Metall Trans A* 12A:1397
15. Hall EL, Briant CL (1985) *Metall Trans A* 16A:1225

16. Sahlaoui H, Makhoulf K, Sidhom H, Philibert J (2004) *Mater Sci Eng A* 372:98
17. Bruemmer SM, Charlot LA (1986) *Scr Metall* 20:1019
18. Stickler R, Vinckler A (1961) *Trans Am Soc Met* 54:362
19. Gao Y (2009) PhD thesis, Loughborough University
20. Bruemmer SM, Arey BW, Charlot LA (1992) *Corrosion* 48:42
21. Robson JD (2004) *Acta Mater* 52:4669
22. Perez M (2005) *Scr Mater* 52:709
23. Zener C (1949) *J Appl Phys* 20:950
24. Raj B, Saroja S, Laha K et al (2009) *J Mater Sci* 44(9):2239. doi: [10.1007/s10853-008-3199-4](https://doi.org/10.1007/s10853-008-3199-4)
25. Radiguet B, Etienne A, Pareige P, Sauvage X, Valiev R (2008) *J Mater Sci* 43(23–24):7338. doi: [10.1007/s10853-008-2875-8](https://doi.org/10.1007/s10853-008-2875-8)
26. Saha R, Ray RK (2008) *J Mater Sci* 43(1):207. doi: [10.1007/s10853-007-2139-z](https://doi.org/10.1007/s10853-007-2139-z)
27. Janis J, Nakajima K, Karasev A, Shibata H, Jönsson PG (2010) *J Mater Sci* 45(8):2233. doi: [10.1007/s10853-009-3908-7](https://doi.org/10.1007/s10853-009-3908-7)
28. Alyousif OM, Engelberg DL, Marrow TJ (2008) *J Mater Sci* 43(4):1270. doi: [10.1007/s10853-007-2252-z](https://doi.org/10.1007/s10853-007-2252-z)
29. Gautam J, Petrov R, Kestens L, Leunis E (2008) *J Mater Sci* 43(11):3969. doi: [10.1007/s10853-007-2292-4](https://doi.org/10.1007/s10853-007-2292-4)